3D Non-Rigid Motion Modeling of the Liver from Undersampled Golden-Radial Phase Encoding (G-RPE) Acquisitions

C. Buerger[1], A. P. King[1], T. Schaeffter[1], and C. Prieto[1]
[1]Division of Imaging Sciences and Biomedical Engineering, King's College London, London, United Kingdom

INTRODUCTION: Motion models derived from MRI have become a valuable tool for respiratory motion compensation in several applications, such as radiotherapy treatment planning [1] or X-ray guided cardiac catheterizations [2]. However, MR-based motion modeling of abdominal organs remains a challenge due to the large non-rigid deformations caused by respiratory motion [3] and the difficulty of acquiring multiple respiratory phases in 3D with adequate contrast and spatial resolution for accurate motion estimation. Recently, the retrospective reconstruction of multiple 3D near motion-free respiratory phases from free-breathing acquisitions has been shown using a Golden-Radial Phase Encoding (G-RPE) trajectory [4,5]. In this work we combine this acquisition scheme with an SSFP contrast to reconstruct multiple images with both adequate contrast and high spatial-temporal resolution. This acquisition provides one high quality image for the most frequent respiratory position as well as several images at different respiratory positions with any arbitrary respiratory resolution (i.e. number and size of respiratory phases, also called bins). These images allow us to apply accurate non-rigid motion modeling of the abdominal tissue deformation.

METHODS: ***1) Acquisition and Reconstruction:*** G-RPE combines Cartesian sampling in the readout direction k_x with an undersampled radial-like scheme in the phase encoding plane (k_y,k_z), having an angular step between consecutive profiles of 111.25^o given by the Golden ratio (Fig 1a). A self-gated respiratory signal is obtained from the central k-space spokes, which are acquired along with each radial profile (Fig 1a-b). G-RPE allows the flexibility to reconstruct several images I_i at any arbitrary respiratory position or bin B_i (i=1...N), by selecting different radial profiles according to their position in the respiratory cycle (Fig 1c). To ensure that each I_i has enough quality to be registered, a maximum angle α_i in the trajectory of I_i is applied as registration quality measure, similar as in [6]. Simulations showed that images reconstructed using non-Cartesian iterative SENSE [6] require an angle of $\alpha_i < 6.25^o$ to ensure enough quality for registration, not necessarily satisfying the Nyquist criterion.

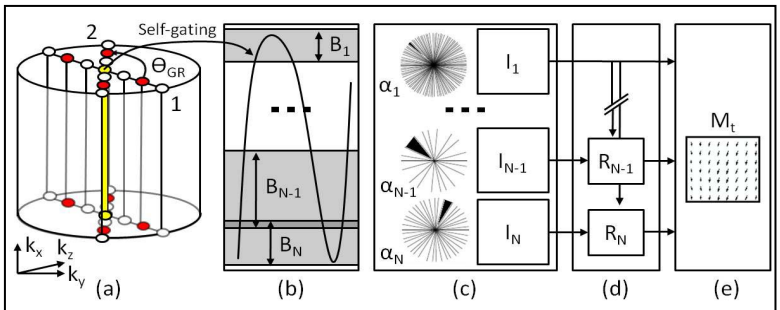

Fig. 1: (a) Golden-Radial Phase Encoding trajectory. (b) Rebinning of the respiratory signal into N bins B_i. (c) Reconstructions I_i at N respiratory positions. (d) Non-rigid image registrations between the high quality phase I_1 and all other phases. (e) Motion modeling allows us to predict an image M_t at any phase between exhale and inhale.

2) Motion modeling: We apply a non-rigid intensity-based registration algorithm [7] to compute the registrations R_i which align the features of the highest quality image I_1 at the most visited respiratory position (most commonly at end-exhale) with the features of all other phases i (Fig 1d). These registrations are used to model the complete respiratory cycle with multilevel B-Splines [8] allowing us to predict an image M_t as a deformation of I_1 at any arbitrary respiratory position t between end-exhale and end-inhale.

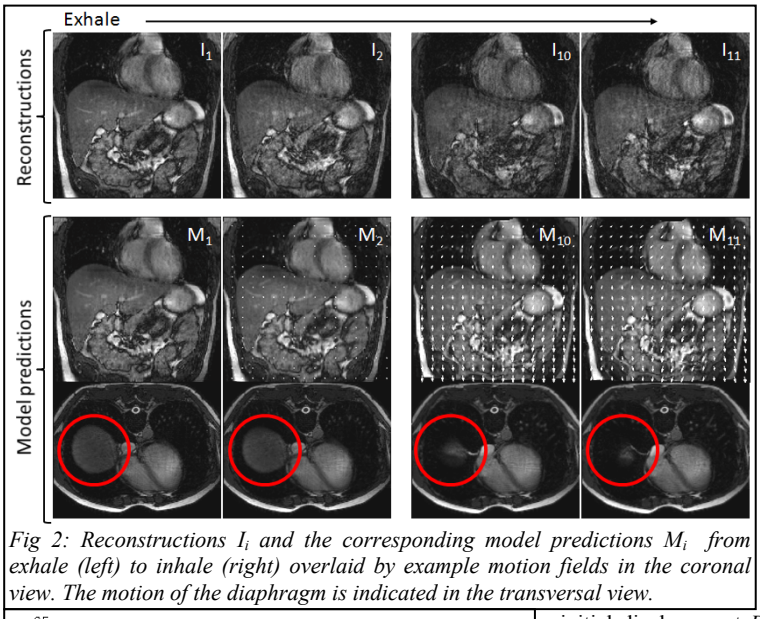

Fig 2: Reconstructions I_i and the corresponding model predictions M_i from exhale (left) to inhale (right) overlaid by example motion fields in the coronal view. The motion of the diaphragm is indicated in the transversal view.

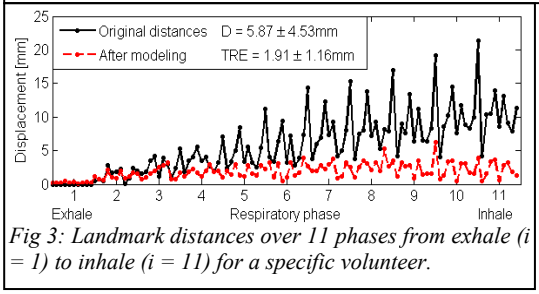

Fig 3: Landmark distances over 11 phases from exhale (i = 1) to inhale (i = 11) for a specific volunteer.

3) In-vivo experiments: Five healthy volunteers were scanned on a 1.5T Philips scanner using a 32-channel coil and the proposed method. Relevant sequence parameters include: balanced SSFP sequence, FOV = 287mm^3, *isotropic resolution = 1.75mm^3*, *TR/TE 3/1.43ms*, *flip angle 30^o*, *P = 1640* profiles with radial undersampling of *2*, scan duration *t = 6.8min*. For each volunteer, *N = 9-11* respiratory phases were reconstructed from exhale (I_1) to inhale (I_N).

RESULTS: Fig 2 (top) shows two exhale (I_1, I_2) and two inhale phases (I_{10}, I_{11}) in coronal view from a sequence of *N = 11* reconstructions of a single volunteer. Although image quality decreases from exhale to inhale due to increased undersampling artifacts, our image quality measure α_i ensures sufficient quality of I_i for registration. The corresponding model predictions M_i at the same respiratory positions overlaid by example motion fields are shown in Fig 2 (bottom) for coronal and transversal views. Image quality now is highly improved since each M_i is a deformation of I_1.

To validate the accuracy of the deformations, for each image pair (I_1,I_i) we manually defined *10* landmark correspondences at anatomical structures within and around the liver. As a measure of deformation accuracy, we computed the target registration error (*TRE*), i.e. the mean distance between the landmarks in M_i and those in I_1, before and after deformation. Fig 3 shows the original and the model-deformed landmark distances for the same volunteer. Over all 5 volunteers, we observed an initial displacement D = 4.36 ± *3.43mm,* and our motion estimations achieved an accuracy of *TRE = 1.83 ± 1.22mm*.

CONCLUSIONS: We applied a non-rigid motion modeling technique to retrospective and self-gated reconstructions of multiple respiratory phases of the abdominal region from free-breathing MRI acquisitions. Accurate model predictions have been shown with an overall error of *1.83 ± 1.22mm.* As future work we will investigate the use of different motion surrogates (e.g. motion of the diaphragm, chest, belly or body surface) that can be extracted from the 4D images to steer the motion model.

REFERENCES: [1] Rohlfing et al, Med. Phys. 2004. [2] King et al, MedIA 2009. [3] Shimizu et al, Radiother. Oncol. 1999. [4] Prieto et al, ISMRM 2009. [5] Buerger et al. ISMRM 2010. [6] Pruessmann et al, MRM 1999. [7] Buerger et al. ISBI 2010. [8] Lee et al. IEEE Trans. Vis. Comp. Graph. 1997.